

Genetic Algorithm-Based Calibration of PV System Parameters Utilizing Deep Learning Architectures

Huihui Tian

School of Ocean Engineering, Yantai Institute of Science and Technology, YanTai 265600, China.

E-mail: huihui202403@126.com

Keywords: power system, machine learning, genetic algorithms, auto-calibrated algorithms, photovoltaic systems, parameter estimation, digital Simulation

Received: June 26, 2025

This study introduces a new method for optimizing evolutionary algorithms to learn characteristics of unknown solar energy systems or subsystems. When used together, Genetic Algorithm (GA) and Deep Learning methods allow for precise PV system calibration. By combining GA's optimization powers with deep learning models' pattern recognition abilities, this technique achieves precise system calibration by fine-tuning model parameters. One way to create a connection between variables like irradiance, temperature, and voltage, which are input parameters, and variables like power production or defect detection, is to employ a model that uses deep learning, and brain networks in particular. Feature extraction is a strong suit of CNNs, making them a promising tool for image analysis in the context of spatial pattern defect detection. Using GA, one may optimize the settings of either the PV system or the deep learning model. To do this, one must define a fitness function that represents the target performance metric. This metric might be anything from maximizing power production to reducing prediction error. In order to decrease the discrepancy between the expected and actual electrical output, GA may optimize the biases and weights of a neural network. To sum up, optimizing and calibrating PV systems has never been easier than with the help of a genetic algorithm and deep learning. Together, these things have the potential to make solar energy systems more efficient, provide better results, and enhance model accuracy. This method optimizes seven parameters of a PV system based on observed PV power: nominal power, tilt, azimuth, albedo, irradiance, temperature dependence, and the DC/AC ratio, which is the proportion of nominal module power to nominal inverter power. Through the optimization of these parameters, a digital twin is generated that faithfully mimics the real characteristics and actions of the unidentified solar power plants or subsystems. In order to create this method, we used data on the PV system's on-site power output, surrounding temperature, and irradiance as collected by satellite in southwest Germany. Here, we provide a method that, when applied to nominal power, produces a mean bias error of around 10%, 3° for azimuth with tilt angles, a temperature coefficient ranging from 0.01% to 0.09%, and now-casts having an accuracy of about 6%. As a conclusion, we provide a novel approach to properly parametrize and model PV systems with little to no prior information about their characteristics and elements.

Povzetek: Študija predstavlja novo metodo, ki z genetskimi algoritmi in globokim učenjem izboljšuje modeliranje in učinkovitost sončnih energetskega sistemov.

1 Introduction

Power system models are used to depict the constantly changing actions of elements of power infrastructure, such as generators, transformers that are and loads. Also, these models help with choices that impact both short-term and long-term planning, as well as real-time operations, and they encourage research into big power system networks. The power system might be severely impacted by inaccurate models that lead to overestimation or underestimation [1], [2]. The power system is now experiencing significant changes due to the increasing use

of sources of renewable energy, smart loads, and mid-size generators. Increasing complexity and stochasticity in the power system might render standard research useless and create enormous operational difficulties [3], [4], [5]. So, in order to validate accurate modeling, recent criteria are stabilizing. Power distribution and dynamic mathematical models are included in Reliability MOD for all operating systems. Validation is necessary every five years for models with capacities over 75 MVA for plant facilities and 20 MVA for individual units. On the other hand, the Western Electricity Coordinating Council (WECC) reduced the model validation barrier to 10 MVA for individual units and 20 MVA for plant facilities, with

validation requirements every five years. Recent years have seen the introduction of mathematical disturbance-based methods. Phasor Measurement Units (PMUs) and other dynamic disturbance recording data are used in these approaches. PMUs, which have lately been installed throughout the bulk power electric systems of many nations, provide more comprehensive measures linked to the grid and are therefore one of the most crucial measuring devices for the future of power systems [6]. PMUs record the plant's reaction to transmission level grid disruptions, such as generator failures, losses, or breaker operations, via continuous high-speed monitoring. Authors validated that the device model using PMU data without powering down the device. The key challenge that confronts this technique and software tools is having several solutions that may exist for the same model performance after conducting the calibration process, therefore finding the real parameter set is sometimes challenging. Furthermore, the resulting set of parameters could differ for different occurrences, even though this approach can provide a one-of-a-kind solution computed using the least square technique for a specific event. In order to make the power system more reliable, it is recommended to use PMU data for model validation and calibration on the power system network. In comparison to testing each machine independently [7], [8], the data acquired by PMU is more realistic and provides a more precise description of the operating range for each element, which is one of its primary advantages. Consequently, if a solid model has been created, this might improve asset usage. Equipment misoperation or failure might be anticipated based on PMU data modeling; a maintenance plan could then be put in place to avoid the failure. In order to calibrate the model, these approaches often rely on many disturbances. Various disturbance events may be applied to the same model in order to identify the optimal solution. There is no assurance that these approaches will discover an ideal answer, even though many events will aid in reducing the number of different options. Another factor that might affect the best solution's dependability is the length of time between disturbance occurrences; this is because these events could alter the power system model's characteristics [9], [10], [11], [12].

Given the critical need for efficient, scalable, and trustworthy verification of models and calibrated approaches, this study presents a technique for calibrating power systems utilizing machine learning algorithms and disturbance data from PMUs. In this thesis, we primarily aim to assess the practicality of machine learning in general techniques for power system calibration using simulated information.

Section 2 provides an overview of the case study and the technique used for PV modeling. Section 3 delves into the suggested methodology for defect identification and the

metrics used to evaluate it. The findings from the PV modeling and the assessment of the proposed fault detection method are presented in Section 3. Part 4 presents a comparison study, evaluating the suggested strategy with current methods. In Section 5, we outline the conclusions that may be drawn from this study.

2 Related work

Authors in [13], the authors assessed their proposed approach for dial reading identification by using 528 images of meter readings. They found that their method attained an accuracy rate of 98.49%. In addition, the influence of a number of different circumstances on the inaccurate readings produced by the electricity meter is explored. According to the results, the most accurate level of accuracy for estimating the inaccuracy of the electricity meter can be attained with a memory length that falls between 600 and 1,200 and a line loss error that is less than 5%. On the other hand, it is advisable to get rid of measurement information that was acquired when the load was relatively light. This will help save time and avoid inspections that are totally unnecessary. The results of the experiments demonstrate that the strategy that was presented is effective in removing the influence of past measurement data regarding the estimation of the error parameter, which ultimately leads in a much more accurate forecast. When it comes to calculating meter faults, the option to change the memory length enables live monitoring and ensures that real-time performance is maintained. There is a certain amount of reference significance that this research has in order to achieve online verification and control of gateway meter flow in the power system.

LPRMNet and SurrogateNet are two distinct deep neural network designs that were used in the training of the machine learning models that were provided by the authors of [14]. The testing error for the models is 3% and 1%, respectively, according to the models. These models have a number of potential applications, including the reduction of bias between determined while suggested power distributions within the core, the highly accurate determination of the nuclear end of life for LPRMs, the capacity for virtual sensing over bypassed or malfunctioning LPRMs, and the on-demand virtual calibration of detectors among successive calibrations.

The authors of [15] were the ones who first measured the direct current element in a distribution system that was established at 10 kV. Following that, a method that makes use of Random Forest Classification with Long Short-Term Memory was proposed as a means of achieving the reverse extraction of the CT distorted current when direct current bias was present. Under conditions of direct current bias, this method necessitates the use of two stages in order to reverse-extract CT-distorted currents. By altering the operating environment of the CT, data samples were generated during the offline stage of

implementation. For the purpose of determining the mapping relationship between the secondary distorted current and the basic component of the main current, they applied the RFC classification system to divide the saturation values of the CT into sub-classes. This allowed them to calculate the mapping relationship accurately. It was determined that PSO-LSTM models were trained for each sub-class. In order to determine which data segments were saturated, the wavelet transform was applied to the secondary current waveform while the online stage was being performed. Following that, these segments were entered into the offline system in order to do the current reverse extraction. The results of the simulation show that the technique that was presented is fairly robust to a wide variety of CT settings and is able to effectively achieve high primary current reconstruction accuracy.

A data-driven self-diagnosis approach was proposed by the authors of [16] in response to the metering errors that were seen in CVTs that were in operation. A synchronized collection of the secondary signals of three-phase CVT outputs is achieved via the use of this technique. Initially, principal component analysis is used in order to extract the residual subspace variables that are responsible for describing the measurement errors. This is accomplished while adhering to the stringent restrictions that are imposed by the operations of three-phase symmetrical electrical systems. Following this, a multidimensional comprehensive assessment is used in combination with bilateral threshold detection in order to determine the boundary conditions of the three-phase CVT's anomalous overall error state and the direction in which it is deteriorating. Last but not least, the learning vector quantized classifier is used in order to rapidly identify the deterioration of CVT measurement inaccuracy by using the results of the coded multidimensional detection. The experimental results reveal that the recommended approach is able to correctly identify error fluctuations at a rate of 0.02%. This is demonstrated by the fact that the technique detects CVT amplitude error overshoots with an accuracy of 0.1%. With this technique, it is possible to accurately identify the problematic phases and the direction of error worsening in real-time, which is necessary in order to fulfill the need for self-diagnosis for CVT metrological flaws at the 0.2 rate.

A thermal neutron detection system that is based on SPND has been developed by researchers from department [17]. The heat route of their nuclear research reactor provided the location for the installation of such detector. Through the use of a current mode chain that employs electrometers that do not include HV, they have recorded the current values for each detector throughout the course of time. We were able to carry out real-time neutron flux measurements during the course of boron neutron capture treatment or boron neutron therapy

because the different materials that were utilized to construct the SPND detectors were selected by hand for that particular reason. During the testing process, the detectors were exposed to a power of four megawatts, which is equal to a neutron flux of $109 \text{ nanocm}^{-2} \text{ s}^{-1}$. As a result of a precise calibration of the thermal neutron spectra, ^{103}Rh -SPND has been shown to be advantageous for the online monitoring of thermal neutron flux on patients undergoing BNCT.

With the intention of making online T_j monitoring more convenient, the authors of [18] developed an intelligent gate driver that is tailored exclusively for SiC MOSFETs. The turn-on delay time is an example of a thermally sensitive electrical variable that may be used so that an online T_j estimate can be generated. In addition to all of this, the accuracy of the measurements is improved by a gate resistance control unit that has a sensitivity improvement that is 10 times more than the original. In the next stage, an online turn-on period measurement system with a resolution of 200 picoseconds and a basis in edge detection will be included into the gate driver. Utilizing a DPT platform to get the calibration curves offline is the most important step in this process. The construction of a half-bridge inverter that is based on SiC is also done in order to provide further evidence of how well the online junction temperature monitoring system operates. Additionally, when the inverter is operating, that intelligent gate driver is able to make an accurate prediction about the junction temperature of the devices.

A unique paradigm for state estimation is offered by the authors of [19], who investigated the measurement chain modeling of phasor measurement units and supervisory control in addition to information collection. This paradigm is based on the concept of adaptive SE. As opposed to passively combating or disregarding the unknown measurement errors statistics, it actively acquires information about them and modifies the structure and parameters of the estimator in real time in order to enhance the accuracy of the state estimates. Without doing field tests, the approach that has been described has the potential to capture measurement error distributions that are arbitrarily complex. This is accomplished while maintaining a high level of computational efficiency and adjusting to abrupt large errors. A sensor calibration plan may also be implemented for both PMUs and SCADA thanks to this capability. Comprehensive SCADA and PMU measurement chain modeling results in measurement mistakes that are both complex and time-varying. The approach that was provided is used to evaluate these measurement errors on the IEEE 30-bus test system before being implemented.

Those who authored [20] proposed procedures that are labor-intensive and costly. One of these ways is phased testing. A PMU-based system that makes use of online measurements without disrupting the operation of generators is an option that is both more economical and

scalable, and it fits the requirements set out by the North American Electric Reliability Corporation. The findings of the research provide a PMU-based framework for verifying and calibrating model parameters. The approach is based on a unique iterative deep learning implementation. The data make it abundantly evident that the proposed technique is capable of properly calibrating power plant models after a single disturbance event. Furthermore, this can be accomplished without the immediate need of knowledge on the model's beginning features. An extensive number of calibrated variables have been used in order to validate the suggested method on both real-world and simulated scenarios, and the results have shown an average degree of error of 1.43 percent.

3 Materials and method

A. Problem statement

Photovoltaic plants and other renewable energy sources are highly weather-dependent and notoriously unpredictable. In order to estimate the power produced by a solar production system, this study suggests a technique for developing a parameterized model. A genetic algorithm is used in the suggested approach to ascertain the optimal mathematical model that corresponds to the produced power's behavior throughout the day. In addition, a mathematical model for estimating harmonic distortion is created using the same process. This model enables one to forecast both the quantity and quality of the generated electricity. The availability, resilience, and dependability of electricity grids depend on precise device modeling. Correct modeling is essential for many important activities, including planning and even making choices about operations in real time. This study introduces a method for calibrating power system

Figure 1: A general technique for optimizing parameters of PV systems. There are little dotted lines that show how the program components interact with each other. The measured PV power information is shown by large dotted lines. Additional input data, shown by continuous lines, includes weather conditions.

C. Calibration power system parameters

(i). DC Power

Following the instructions in, the second step is to determine the temperature of the PV modules. Along with the SolarGIS ambient temperature, there is an irradiance-dependent value:

$$T_{mod} = T_{amb} + 25K \left(\frac{G}{1000 \text{ W/m}^2} \right) \quad (1)$$

where T_{mod} is the module temperature, T_{amb} is the temperature outside, while G is the amount of light reaching the array's surface. As previously said, Equation

model parameters using deep learning. Mathematical techniques that form the basis of current calibration procedures are ill-posed, meaning that they may have more than one solution. Applying a deep learning architecture trained to estimate model variables from simulated Phasor Measurement Unit information is how we're attempting to tackle this challenge.

B. Overall system model

Optimal performance of the PV system parameters is achieved by executing the procedures outlined in each stage of the technique, as seen in Figure 1. This involves integrating measured and meteorological data as inputs. This section provides an extensive synopsis of all the techniques and data utilized throughout the essay.

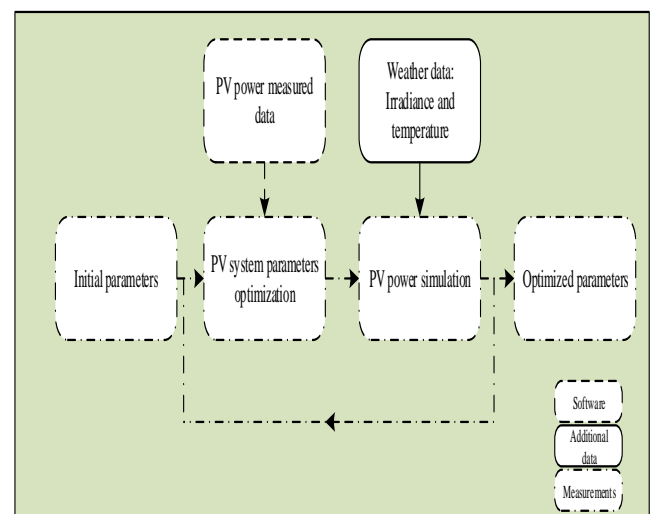


Figure 1: System model

() is oversimplified and fails to account for the speed and direction of the wind in addition to varied PV module technology.

According to Heydenreich et al., one may determine the temperature dependence of PV modules and how it relates to irradiance after calculating the module temperature:

$$\eta(G, T_{STC}) = aG + b \ln(G + 1) + c \left(\frac{\ln^2(G+e)}{G+1} - 1 \right) \quad (2)$$

$$\eta(G, T_{mod}) = \eta(G, T_{STC}) (1 + \gamma(T_{mod} - T_{STC})) \quad (3)$$

where T_{STC} is 25°C, η The PV module efficiency under particular conditions is represented by η , the temperature coefficient describing the power or efficiency of the PV module at any given temperature, constants a , b , and c are the three variables that fit the curve of the PV component efficiency behavior at all given irradiance.

The model developed by Heydenreich et al. can accurately reproduce the performance of applicable PV

technologies under low irradiance circumstances, as stated in and confirmed in.

(ii). AC Power

Finally, the same technology from earlier articles is used to simulate AC power. Module mismatch, inverter efficiency, inverter power restriction, and AC cable losses are some of the elements that are taken into account separately in that context. Schmidt and Sauer's model is used to model the inverter.

D. Deep learning technique

A CNN with two convolutional layers interspersed by maximum pooling operations and two fully connected layers follows in the deep learning method. More information may be seen in Figure 5. The input layer documents the power system's dynamic reaction to disturbances using time samples for PMU data. These samples document the system's condition just before to the disruption and its reaction thereafter. Variables like rotor speed, rotor angle, and voltages at various buses are included in these replies. A 256-filter, one-dimensional convolutional kernel, sized at a quarter of the input samples, makes up the first convolutional layer. Because of this, it is possible to compare characteristics across the majority of input samples and apply filters accordingly. By applying padding to each filter, we can make sure that their output is exactly identical in size as their input. After that, a corrected linear activation is performed element-wise. In order to reduce the feature size, a max-pooling layer is used to implement a fourfold downsampling method. The second convolutional layer uses a 512-filter setup with a one-dimensional convolutional kernel that is four times the size of the input samples. This enables the application of filters and the comparison of characteristics across several filter responses. By applying padding to each filter, we can make sure that their output is exactly identical in size as their input. After that, a corrected linear activation is performed element-wise. A max-pooling layer is used to implement a two-fold downsampling technique. There are 256 hidden neurons in the first completely linked layer and 1024 in the second.

A connection is established between the first layer and the second convolutional layer's downsampled output. The second completely linked layer takes its input from this layer. In order to avoid overfitting, each layer uses an element-wise corrected linear activation and is followed with a dropout layer having a drop rate of 0.2. The magnitude of the input signals is anticipated to be big, for example, 90 seconds multiplied by 30 samples/second, due to the higher PMU sampling rate of 30 samples/second. Large CNN kernels are required to capture the data's long-term temporal connection. Because of this, the model's performance will be impacted by the huge number of parameters. We discussed this matter by introducing dilated convolution. Figure 4 shows an example of a diluted convolution, which enlarges the convolution kernels through establishing gaps between their adjacent parts. Figure 4 shows that when the model delves deeper, the receptive field grows exponentially due to the strength of the residual blocks and dilated convolution, allowing us to capture more temporal correlations at the same computing cost. The field of reception size may be calculated using the model depth and dilation rate. A receptive field of 4096 samples/second, divided by 30 samples/second, equals 136.5 seconds for a model with a depth of 12 and a dilation rate of 2.

E. PV system parameters optimization

The GA is an evolutionary-inspired method for handling difficult optimization issues. In 1975, Holland was the first to use this evolutionary optimization method to find the global optimal solution to a problem. The advantages of GA optimization include a small data set need, the fact that objective values are not known in advance, and the fact that the formulation of the cost function is simplified due to the lack of a gradient function. Even when a convex function is taken into account, optimization does not provide a global optimal value.

This GA is based only on data collected from weather stations and measurements of PV power production. Following the steps shown in Figure 3, we have created our own GA.

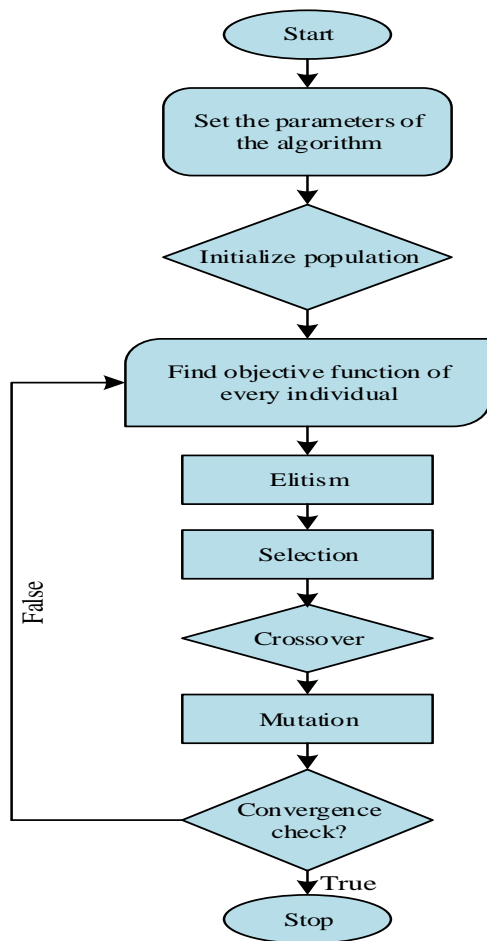


Figure 2: GA Optimization model

The GA optimization procedure is composed of six distinct phases:

- Starting with the starting value to optimize (initial parameters) and a predefined randomness %, the initialization stage generates a vector of possible PV plant configurations (members), populating it with randomly assigned values (population). Depending on the situation, the PV power setup could vary from one component to many.
- Using a loss function that has been developed, the fitness scoring step compares and evaluates each PV plant configuration in the population with the monitoring data. A score is then given.
- If a PV plant configuration has a high score, it has a better chance of being randomly picked and moved on to the next population during the fit selection stage.
- The crossover stage involves the random selection and combination of parameters for a subset of the PV plant designs that emerged from the fitting selection step. A result is that the new

population now includes PV plants with different configurations.

- Variables of the PV plant setups undergo mutations in the mutation stage as a result of a mutation probability that is randomly allocated to each parameter in every next-generation PV power plant configuration.
- It ultimately comes down to repopulating the following population using the characteristics of the optimal PV plant layout from the present population. Once the stop requirements are satisfied, the procedure terminates;

We suggest these two measures to maximize DC PV power optimization. To begin, let's pretend that the installed capacity is 1 kW. Secondly, to get the best fit for each of the three variables from the Heydenreich et al. approach, use cross validation optimization (we test each set of three parameters). Then, to learn about the temperature coefficient, use GA optimization. Here, we compare the generated DC power from PV simulations with the observed power after normalization. Calculated with the settings before developing and optimizing, such as albedo, tilt, along with azimuth angles, simulated PV power DC relies on the direct along with diffuse irradiance in the array plane.

AC Power

We presupposed a PV system with a nominal power of 1 kW p in order to maximize the DC to AC ratio. We used GA to reduce the discrepancy between the AC power output of our simulations and the normalized output of our measurements, drawing on the Schmidt as well as Sauer model. Assuming 1% cabling losses, the optimized parameters are used to compute PV power AC.

By comparing the observed PV power to the simulated AC PV power, GA is then used to optimize the nominal power.

A solar energy system or subsystem's fundamental characteristic may be optimized, and then a digital twin might be built to mimic its present and future behavior by simply adjusting to the current and future weather.

Weather data

Using a sequence of models and a time series of operational parameters (weather data), one can simulate the AC energy yield of a PV system. For the PV power simulation, we utilize SolarGIS's basic meteorological data collection, which is obtained from satellites. For example, weather data collected in southwestern Germany includes global horizontal irradiance (G_hor), diffuse horizontal irradiance, and ambient temperature (T_amb) in a time series format with a precision of 15 minutes for 2017 and the last 90 days of 2016.

PV power measured data

A real-life PV system that has a 5-minute resolution was installed in south-west Germany on January 1, 2010, and the statistics for 2017 and the final 90 days of 2016 are derived from that system. Table 1 displays the fundamental PV power plant characteristics and the initial settings of the simulation parameters. The remainder of the parameters are based on assumptions, whereas the following are retrieved from several sources: azimuth angle, tilt angle, nominal power, and temperature coefficient from the solar panel's datasheet and the design layout, respectively. Table 1 contains the PV parameters that will be used as reported parameters for the remainder of this study.

Initial parameters

Included in the starting parameters is a set of established values for the primary parameters that are required to characterize and model the power output of a generic PV system or subsystem. The GA optimization procedure will begin with these settings as its starting points. The nominal power of the PV system, as well as the angles of tilt and azimuth, the albedo, the irradiance, and the temperature, as well as the DC to AC ratio, are all components that make up the system. To kick off our project, we've settled on the following numbers for our parameters:

- Nominal power = 1 kW
- Tilt angle = 25°
- Azimuth angle = 180° (south oriented)
- Albedo = 0.2
- Temperature coefficient = $-0.43\%/^{\circ}\text{C}$
- DC to AC ratio = 1

Through optimizations carried out in this study, it has been discovered that beginning parameter values do not directly affect the end outcome, but they may decrease the overall computing time.

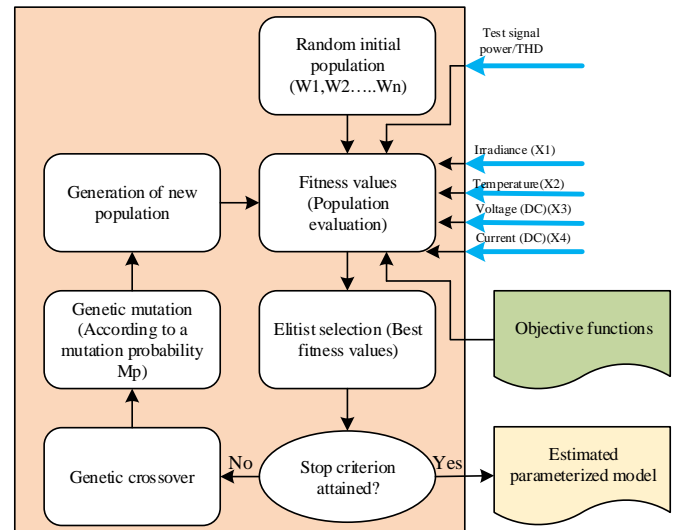


Figure 3: GA model for parameter optimization

F. Principal component analysis

By compressing linked data without substantially reducing information loss, Principal Component Analysis (PCA) simplifies high-dimensional data. By mapping physical variables into a low-dimensional subspace that preserves the majority of their variances, it derives Principal Components that are independent of each other. Downsampling the generated response times from 60Hz to 10Hz was the first step in reducing the size of the chosen features in this study. Applying PCA separately for each feature significantly decreased the features. The mean reconstruction error obtained after PCA was 0.01%, and we utilized almost 200K data to select the top 10 PCs

4 Results & discussion

A. Implementation

A Python API called TensorFlow (<https://www.tensorflow.org/>) is used to build the CNN model. TensorFlow's extensive feature set and strong community backing led to its selection. The UVM DeepGreen cluster, an innovative massively parallel cluster of more than 70 GPUs supporting more than 8 petaflops of mixed precision computations relying on the NVIDIA Tesla V100 design (<https://www.uvm.edu/vacc>), is the primary platform for training and testing all models.

Databases that accurately portray the PV device's operation in actual outdoor settings were then generated using the model of the system. Included in such databases are records depicting ideal functioning and data reflecting purposely generated problems, with profiles of solar irradiance (G) and module temperature (T_m) measured annually. Regular annotating with appropriate class labels is applied to the recorded data during the data creation phase. Of the total raw data samples, 52,385 were used for detection purposes, while 43,624 were set aside for diagnosis. Data dependability and quality were the primary goals of the preprocessing pipeline. This was accomplished by executing the removal of rows with missing values, thereby filtering out undesired data. After that, you may find and maybe remove superfluous information by detecting duplicate rows. Handling outliers in numerical columns became our focus in order to strengthen the dataset's resilience. The data was preprocessed and then divided into two groups: 23,774 for detection and 19,788 for diagnosis. Step two included partitioning the dataset according to characteristics (X) and desired labels (y). The 'System_State' column was used to determine the labels, and the features (X) were created from the columns related to solar irradiance (G), module temperature (T_m), and PV array output power (P_{mp}). The Features set was then standardised with the help of scikit-learn's StandardScaler. By guaranteeing constant feature scaling, this vital step promotes convergence and improves deep learning model performance. Next, the data set's sequential length (num_time_steps) and the total amount of columns (features) were specified. The provided time steps were used to build sequences and related labels in iterations. To create sequences, we looked at a data window that was num_time_steps long. We got 23,575 sequences for the detection dataset, which leaves 19,589 sequences for the diagnosis dataset, and the loop adds these sequences and their labels to separate arrays. The scikit-test split method was used to divide the dataset into three parts: training, validation, and test. Half of the data came from the test set and half from the set used for validation, with the training set making up 70% of the total. 30 samples/sec is the standard sampling rate for PMU measurements. To demonstrate the efficacy and reliability of the suggested approach, two trials were conducted:

B. Experiments

Having a sampling rate of 60Hz, six measurements were taken from the bus that was directly linked to the generator for each occurrence. Speed, terminal voltage, field current, field voltage, and reactive power were all part of the set of measurements. After calculating the standard deviation and eliminating the mean from the measurements, they were normalized and standardized. After merging the six data into one feature vector, principal component analysis was used to decrease the

vector's size from 81,000 to 13,500. 390K simulated response samples remained in the dataset after the removal of unstable samples. Using the training set, the CNN model underwent 200 epochs of training, with each epoch followed by validation on the validation dataset. The optimal model was discovered at epoch #88. Both the training and validation sets have MSEs of 0.048 and 0.016, respectively. There were occurrences in the testing dataset that the trained model did not see. The testing dataset had 19.5K samples in total. For the testing set, the Mean Square Error (0.017) was calculated. The suggested system successfully estimates the values of the model's parameters, according to the experimental findings presented in Table II with Figure 5.

Training a massively parallel deep learning neural networks using the suggested methods yielded a well-posed answer with a very modest MSE of 0.017 on the test set. A single disturbance event is all that is required to precisely calibrate the model variables according to the suggested technique, which does not depend on the initial parameter estimate. It is possible to get even better outcomes with more training data, more complex ensemble models, and more trustworthy modeling in general. It is possible to confirm the calibrated models' outputs by comparing them to the collected PMU data.

- Case studies: Using the same models for power plants, this research dynamically simulated five disturbance episodes. The simulated examples were generated by connecting the playback module to simulated occurrences. These virtual occurrences were generated by simulating actual voltage flicker as well as fluctuation events by frequency and voltage modulation. We use the same model settings for the simulated situations. We mimicked real-world conditions by adjusting the voltage from 500KV on the high-voltage portion of the transformers to 1.1pu, and we kept the frequency within [99.6%, 100.05%] of the power supply fundamental frequency (60Hz). By applying the suggested method to every one of these events independently, we can demonstrate that a single disturbance event is sufficient for calibrating a power plant model, leading to a solution that is almost well-posed. Event replay allows one to compare observed PMU data and model output using calibrated parameters, thereby validating the correctness of the suggested deep learning technique.
- Case studies: To demonstrate the efficacy and resilience of the suggested deep learning method, two real-world disturbance occurrences were used, both measured at the high-voltage end of the transformer from an identical power plant. Since the real model parameters have never been known in reality, the calibrated model is verified by

comparing the observed PMU data and model output via event playback, similar to (1).

C. Evaluation metrics

Mean absolute percentage deviation (MAPD), root mean square deviation (RMSD), mean bias deviation (MBD), along with mean absolute deviation (MAD) are the four metrics utilized to measure the GA optimization's efficacy in this study. The metrics for error are determined using Equations (1) through (4) in that order.

$$RMSD = \sqrt{\frac{1}{n} \sum_{i=1}^n (y_i - x_i)^2} \quad (4)$$

$$MAPD = \frac{100}{n} \sum_{i=1}^n \frac{|y_i - x_i|}{|y_i|} \quad (5)$$

$$MBD = \frac{1}{n} \sum_{i=1}^n (x_i - y_i) \quad (6)$$

$$MAD = \frac{1}{n} \sum_{i=1}^n |y_i - x_i| \quad (7)$$

where y_i is the actual value, x_i where n is the total amount of observations (not including values taken at night) and is the estimated value.

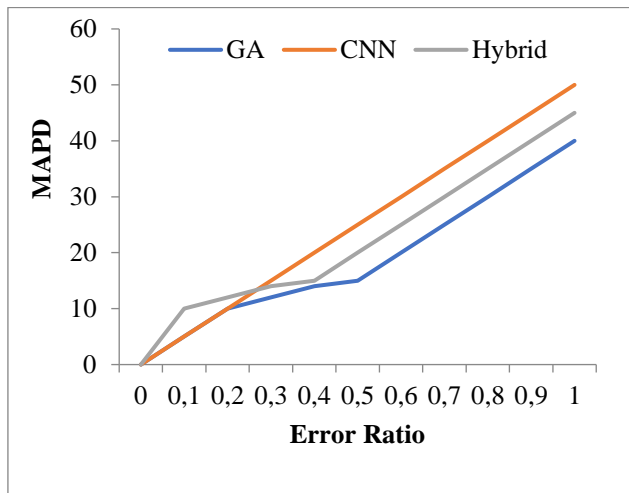


Figure 4: MAPD analysis

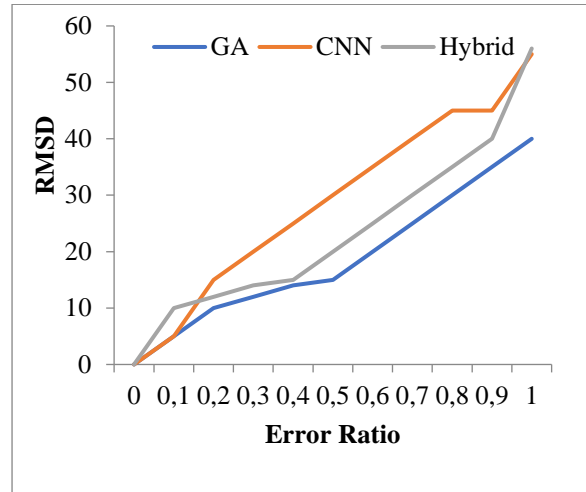


Figure 5: RMSD analysis

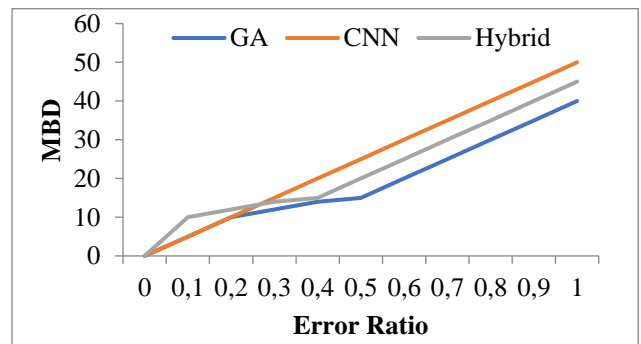


Figure 6: MBD analysis

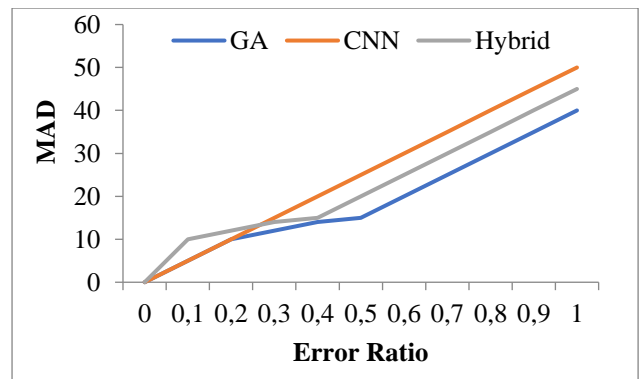


Figure 7: MAD analysis

D. Results

We quantitatively tested the system to show that the CNN could estimate the model variables from the response data gathered by the system. The suggested system's correctness, scalability, and dependability were confirmed via three primary trials. 390K simulated response samples remained in the dataset after the removal of unstable samples. The ratio of the dataset's divisions is 60:20:20, with training, validation, and testing sets each comprising 20%. With each iteration, the model was tested on the validation dataset after being trained for 100 epochs on the training set. The optimal model was discovered at epoch #88. Both the training and validation sets have Mean Square Errors (MSEs) of 0.048 and 0.016, respectively. There are occurrences in the testing dataset that the trained model has never seen before. The testing dataset has a grand total of 19.5K samples. On the testing set, the MSE is 0.017. As shown in Figure 8, the experimental data MMsarized demonstrate that the

suggested system can reliably estimate the values of the model variables. The suggested training process for a massively parallel deep neural network can locate a well-posed solution, as the MSE on the test set is just 0.017.

E. Calibration of power system parameters

Important information for verifying power system equipment was found in the data gathered following system disruptions. We provide a quantitative assessment of the system's performance. Model parameters were estimated with a high degree of precision, with a mean squared error of just 0.017 on the testing dataset. In addition, we guarantee that, using the same architecture, the suggested system is scalable. These encouraging findings, in our opinion, warrant continued investigation and the creation of supplementary tools for variable calibration.

Table 1: Findings from the experiment

| Parameter | MAE | MSE | Parameter | MAE | MSE |
|-------------------------|-------|---------|------------------------------|--------|---------|
| Nominal power | 0.237 | 0.11222 | DC Power | 0.085 | 0.00934 |
| Tilt angle | 0.028 | 0.00544 | Global Horizontal Irradiance | 0.056 | 0.00386 |
| Azimuth angle | 0.154 | 0.02829 | Horizontal Irradiance | 0.085 | 0.00596 |
| Albedo | 0.031 | 0.00173 | Ambient Temperature | 0.012 | 0.00171 |
| Temperature coefficient | 0.085 | 0.01943 | Frequency | 0.0545 | 0.00493 |
| DC to AC ratio | 0.056 | 0.00676 | Phase angle | 0.0616 | 0.00523 |
| AC Power | 0.089 | 0.00896 | Magnitude | 0.026 | 0.01356 |

The above data make it easy to compare the models' prediction abilities. Furthermore, while using various approaches with different meteorological data sources, the anticipated hourly generating intensity would range significantly. The three models with distinct sets of meteorological data are provided in Table 8 along with their average assessment indices. A single disturbance event is all that is required to precisely calibrate the model

variables according to the suggested technique, which does not depend on the initial parameter estimate. It is possible to get even better outcomes with more training data, larger and collaborative models, and more trustworthy modeling in general. Comparing the calibrated models' outputs with the actual recorded PMU data is one way to confirm the accuracy of the models.

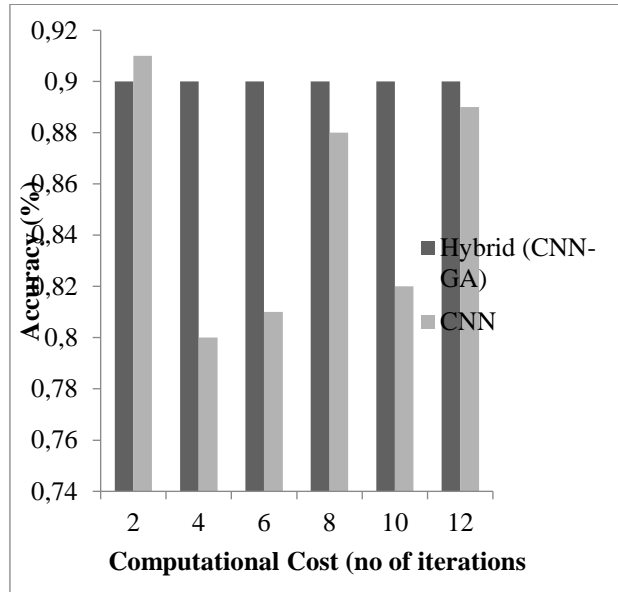


Figure 8: Accuracy analysis

The investigated system takes as input a collection of environmental information gathered from fifty separate sites. Due to differences in local climate and sunshine, plus the fact that only 200 hours of data were evaluated, the results may not be generalizable.

Table 2: The hyperparameter tuning results of hybrid data.

| Model | Layers | Epochs | Learning Rate | Batch Size | MAE | Accuracy (%) | MAPE | RMSE |
|--------|--------|--------|--------------------|------------|--------|--------------|------|-------|
| GA | - | - | - | - | 0.3242 | 85 | 9% | 0.521 |
| CNN | 4 | 200 | 1×10^{-3} | 8 | 0.3907 | 88 | 11% | 0.61 |
| Hybrid | 6 | 200 | 1×10^{-3} | 8 | 0.134 | 95 | 8% | 0.326 |

In order to achieve the increased operational photovoltaic coverage at a low cost and achieve sustained development and competitiveness simultaneously, an accurate solar forecast is seen as crucial. How accurate a model's predictions are depends heavily on the forecasting horizon. In general, a forecasting model's accuracy tends to decline with increasing forecasting horizons. The location of the PV installation affects the quality of the forecast, which diminishes as the forecasting length increases. It is critical to choose the right forecasting models that work with the horizon and the PV installation's location. This paper's primary goal is to investigate how various neural network types affect the reliability of the PV system's power production. If we compare the predicted approaches to the more traditional ones, we see that most of them are hybrids. So, it's clear that hybrid models are superior when it comes to making predictions. They may improve performance indicators while achieving lower ones. Therefore, they can achieve far higher precision. Also, when the weather changes, so does the accuracy of predicting models. Seasons change from nation to country, and it's important to reevaluate the

Consequently, the trained system that is supposed to follow the PV panels won't be able to do a good job in any given location. In contrast, trained neural networks will have a greater understanding of the real environment and be better equipped to deal with weather fluctuations if the dataset is gathered from the same place over an extended period of time. Machine learning along with deep learning-based optimization solutions outperform previous methods in terms of accuracy and adaptability.

Adjusting a deep learning model's hyperparameters allows one to fine-tune its hidden unit, batch size, and epochs, among other things. Keep in mind that the amount of training samples is indicated by the batch size. It is possible to quicken the training pace by adding more samples. Memory constraints will arise if the batch size exceeds a certain threshold. On the other hand, underfitting might occur if the batch size is too small. There are a certain number of parameters indicated by the hidden unit. The likelihood of overfitting increases as the quantity of hidden layer units increases. For each batch, the number of training iterations is represented by an epoch. In order to maximize the loss value, the training curve will decrease as the epoch grows. As a result, we started by fixing the batch size, and we tested three to five layers at each step while adjusting the hyperparameters at the same epochs.

input parameters and climatic conditions as well. So, weather categorization is one of the most important factors for making forecasting models more accurate. As a result, weather classifications must be included in the forecasting process. When the module and ambient temperatures rise, for example, certain forecasting models show greater performance than others, and in partly cloudy or gloomy weather, some show lower error rates. In conclusion, the study's results suggest that the input parameters' quantity and type, the forecast horizon's duration, and the hybrid models' and methodologies' performance enhancement claims are true. Compared to more basic and traditional machine learning models, the accuracy should take precedence. This study provides future researchers, planners, and professionals in photovoltaics with the most up-to-date information and a comparative examination of machine learning algorithms to help them enhance the performance of forecasting models. It may be feasible to enhance the performance of PV systems and reduce reliance on traditional energy sources by using accurate tools and methodologies for PV power forecasting. The exponential growth of new

machine learning theory may be attributed, in part, to the use of supervised neural networks in forecasting, which are capable of massive data processing and nonlinear representation.

5 Conclusion

Using PMU disturbance data, this study demonstrates a new method for calibrating the parameters of dynamic models. Estimating parameters of various models in various systems learned from a large quantity of simulated data has been accomplished with extremely good accuracy using the suggested method. In order to discover the best solution for the estimation of parameters issue, the suggested system combines deep learning methods with current computational power system modeling tools. The suggested technology outperformed theoretically based approaches to parameter calibration in this study. To improve the stability and dependability of power systems, it is critical to assist engineers in real-time in calculating the necessary reactions. In the future, we will look at ways to enhance these findings in complex topologies, such as by modeling the complicated kind of generators in a large power system with additional buses while employing reinforcement learning.

References

- [1] Wang, Y., Zhai, B., Gao, S., Guo, Y., Shen, C., Chen, Y., Zheng, Z., & Song, Y. (2025). Data-Driven Parameter Calibration of Power System EMT Model Based on Sobol Sensitivity Analysis and Gaussian Mixture Model. *IEEE Transactions on Power Systems*, 40, 1024-1036. <https://doi.org/10.1016/j.xcrp.2025.102624>
- [2] Wang, L., & Qi, J. (2024). Parameter Subset Selection for Power System Model Calibration Using Both Sensitivity and Identifiability. *IEEE Access*, 12, 153783-153795. DOI:10.1109/ACCESS.2024.3481318
- [3] Owolabi, A.B., Yahaya, A., Yakub, A.O., Same, N.N., Amir, M., Adeshina, M.A., & Suh, D. (2025). Hybrid Deep Learning Models for Power Output Forecasting of Grid-Connected Solar PV Systems: A Monocrystalline and Polycrystalline PV Panel Analysis. *International Journal of Energy Research*. <https://doi.org/10.3390/en16124645>
- [4] Andal, C.K., & Jayapal, R. (2023). Intelligent Power and Cost Management System in Small-Scale Grid-Associated PV-Wind Energy System Using RNN-LSTM. *SN Computer Science*, 4. DOI: <http://doi.org/10.11591/ijpeds.v12.i4.pp2531-2544>
- [5] Acilan, E., & Gol, M. (2022). Identifiability Analysis for Power Plant Parameter Calibration in the Presence of Collinear Parameters. *IEEE Transactions on Power Systems*, 37, 2988-2997. DOI: 10.1109/TPWRS.2021.3130076
- [6] Lu, X., Shi, D., Zhu, B., Wang, Z., Luo, J., Su, D., & Xu, C. (2017). PMU assisted power system parameter calibration at Jiangsu electric power company. 2017 IEEE Power & Energy Society General Meeting, 1-5. DOI: 10.1002/anie.202103557
- [7] Aljundi, A., Mohamed, O., & Abu Elhaija, W. (2025). Calibration of parameters and predictive control strategy of a wind turbine for improvement of energy harvesting. *Proceedings of the Institution of Mechanical Engineers, Part A: Journal of Power and Energy*. <https://doi.org/10.1177/09576509251318175>
- [8] Wang, S., Diao, R., Xu, C., Shi, D., & Wang, Z. (2021). On Multi-Event Co-Calibration of Dynamic Model Parameters Using Soft Actor-Critic. *IEEE Transactions on Power Systems*, 36, 521-524. DOI: 10.1109/TPWRS.2020.2990179
- [9] Kalsi, K., Sun, Y., Huang, Z., Du, P., Diao, R., Anderson, K.K., Li, Y., & Lee, B. (2011). Calibrating multi-machine power system parameters with the extended Kalman filter. 2011 IEEE Power and Energy Society General Meeting, 1-8. doi:10.1109/PES.2011.6039224
- [10] Huang, R., Fan, R., Yin, T., Wang, S., & Tan, Z. (2019). Parameters Calibration for Power Grid Stability Models using Deep Learning Methods. *arXiv: Signal Processing*. <https://doi.org/10.48550/arXiv.2109.12811>
- [11] Khazeinyasab, S.R., Zhao, J., Batarseh, I., & Tan, B. (2022). Power Plant Model Parameter Calibration Using Conditional Variational Autoencoder. *IEEE Transactions on Power Systems*, 37, 1642-1652. DOI: 10.1109/TPWRS.2021.3107515
- [12] Wshah, S., Shadid, R., Wu, Y., Matar, M., Xu, B., Wu, W., Lin, L., & Elmoudi, R. (2020). Deep Learning for Model Parameter Calibration in Power Systems. 2020 IEEE International Conference on Power Systems Technology (POWERCON), 1-6. DOI: 10.1109/POWERCON48463.2020.9230531
- [13] Li, C., Wang, H., Shen, H., Yang, P., Wang, Y., Li, Q., Li, C., Li, B., Guo, R., & Wang, R. (2023). Online verification and management scheme of gateway meter flow in the power system by machine learning. *PeerJ Computer Science*, 9. <https://doi.org/10.1016/j.xcrp.2025.102624>
- [14] Tunga, A., Heim, J., Mueterthies, M., Gruenwald, T., & Nistor, J. (2024). AI Enabled Neutron Flux Measurement and Virtual Calibration in Boiling Water Reactors. *ArXiv*, abs/2409.17405. <https://doi.org/10.48550/arXiv.2409.17405>
- [15] Dang, S., Xiao, Y., Wang, B., Zhang, D.Q., Zhang, B., Hu, S., Song, H., Xu, C., & Cai, Y. (2023). A High-Precision Error Calibration Technique for Current Transformers under the Influence of DC

- Bias. Energies.
<https://doi.org/10.1016/j.electacta.2019.135325>
- [16] Zhang, Z., Lu, H., Li, B., & Ding, L.J. (2024). Research on Data-Driven Self-Diagnosis for Measurement Errors in Capacitor Voltage Transformers. *IEEE Transactions on Instrumentation and Measurement*, 73, 1-12. <https://doi.org/10.1016/j.jcis.2025.137322>
- [17] Fares, M., Messai, A., Mameri, S., Messaoudi, M., Debili, M.Y., Nourddine, H., Negara, K., & Samir, B. (2021). Development of self-powered neutron detectors used in nuclear medicine for the measurement of neutron flows during treatment of boron neutron therapy. *Radiation Detection Technology and Methods*, 5, 459 - 465. DOI:10.1007/s10967-020-07446-5
- [18] Qiao, L., Wang, F., Dyer, J., & Zhang, Z. (2020). Online Junction Temperature Monitoring for SiC MOSFETs Using Turn-On Delay Time. 2020 IEEE Applied Power Electronics Conference and Exposition (APEC), 1526-1531. DOI: 10.1109/TPEL.2021.3072436
- [19] Cheng, G., & Lin, Y. (2024). Power System Adaptive State Estimation in Unknown Measurement Environment. *IEEE Transactions on Instrumentation and Measurement*, 73, 1-17. DOI:10.1109/TIM.2024.3403203
- [20] Matar, M., Xu, B., Elmoudi, R., Olatujoye, O., & Wshah, S. (2022). A Deep Learning-Based Framework for Parameters Calibration of Power Plant Models Using Event Playback Approach. *IEEE Access*, 10, 72132-72144. DOI: 10.1109/ACCESS.2022.3188313

